Cancer Chemother Pharmacol (2011) 67:813–821
DOI 10.1007/s00280-010-1387-9

ORIGINAL ARTICLE

Solamargine, a steroidal alkaloid glycoside, induces oncosis in human K562 leukemia and squamous cell carcinoma KB cells

Lingmei Sun · Ying Zhao · Huiqing Yuan · Xia Li · Aixia Cheng · Hongxiang Lou

Received: 21 April 2010 / Accepted: 7 June 2010 / Published online: 19 June 2010

Abstract
Purpose The aim of this study was to demonstrate that solamargine (SM) mediates its cytotoxicity via oncosis.
Methods The cytotoxicity of SM on cancer cells was examined by 3-(4,5-dimethylthiazol)-2 and 5-diphenyltetrazolium bromide assay. Cell membrane integrity was assessed by detecting the leakage of cytoplasmic content, the release of lactate dehydrogenase (LDH), and the uptake of propidium iodide (PI). We use whole-cell recording to measure the time courses of membrane blebbing and disruption in human K562 leukemia and squamous cell carcinoma KB cells. The effects of SM on cytoskeletal systems were detected by Western blotting and immunofluorescence.
Results The cytotoxicity of SM did not correlate with the expression level of the multidrug resistance MDR1 and was triggered rapidly by 10 μM SM (5 min caused 50% maximum cytotoxicity). Its rapid ability to make propidium iodide (PI) permeate into tumor cells, LDH release, and leakage of cytoplasmic content at the same rate (within minutes), suggests a killing mechanism that involves plasma membrane perturbation. SM induced membrane blebbing within 5 min of sustained application. Both chelating extracellular calcium with EGTA and clamping intracellular calcium concentrations with a high concentration of the cell-permeable chelator BAPTA-AM did not prevent blebbing. Polyethylene glycols having molecular weights ≥3,350 blocked membrane blebbing. SM also disrupted the cytoskeletal systems: degradation of microtubules and actin proteins.
Conclusion SM can rapidly initiate acute injury and bursting by damaging to cellular membrane and may offer a novel therapeutic strategy in treatment of cancer.

Keywords Alkaloidal saponins · Solamargine · Membrane blebs · Microtubule · Actin

L. Sun · Y. Zhao · A. Cheng · H. Lou (✉)
School of Pharmaceutical Sciences, Shandong University,
No. 44 West Wenhua Road, Jinan, China
e-mail: louhongxiang@sdu.edu.cn

H. Yuan
Department of Biochemistry and Molecular Biology,
School of Medicine, Shandong University,
No. 44 West Wenhua Road, Jinan, China

X. Li
School of Ocean, Shandong University, Weihai, China

Introduction

The patterns of cellular reaction to injury leading to cell death are important in the understanding and recognition of toxic and other types of injury. At the present time, two types of prelethal reaction have been characterized: apoptosis and oncosis [1]. Oncosis, derived from the Greek word "swelling", is the common pattern of change in infarcts and in zonal killing following chemical toxicity [2]. In this reaction, the earliest changes include marked alteration in cell shape and volume, frequently occurring within seconds to minutes following application of the injury. More specifically, the cells often exhibit blebs, mitochondria undergo rapid swelling, nuclear chromatin clumping, and the elements of the cytoskeleton, including actin and tubulin, are markedly altered [1, 3]. In contrast, apoptosis is defined as an active, fixed-pathway process of cell death characterized by cell shrinking, cytoplasmic condensation, ladder DNA degradation, and nuclear fragmentation resulting in the formation of apoptosis bodies

[4]. Today, however, apoptosis and oncosis are no longer believed to be mutually exclusive processes [5] and, moreover, apoptosis is probably not the only or even the main mechanism by which tumor cells are killed by anticancer drugs or radiotherapy [6]. It is accepted that apoptosis and oncosis share certain mechanisms and alterations such as loss of mitochondria permeability and membrane potential, and that cell fate is mostly due to the intensity and duration of the death signal and the cell genetic and metabolic status [7–10].

Natural products provide a great chemical structural diversity. In this respect, steroidal alkaloidal saponins are thought to be an important component of the plant's chemical armory against herbivores and microbial pathogens in wild species [11]. Also, steroidal alkaloidal saponins have been demonstrated to have strong cytotoxicity and induce apoptosis to cancer cell [12, 13]. Solamargine (SM, Fig. 1), isolated from *Solanum incanum* herb, was a steroidal alkaloidal saponin. It has potent cytotoxic activity in vitro against cell lines from solid tumors including colon (HT-29, HCT-15), prostate (LNCaP, PC-3), breast (T47D, MDA-MB-231), and human hepatoma (PLC/PRF/5) cells [14–16]. As reported in the literature, SM is able to induce cell death through apoptosis by triggering human tumor necrosis factor receptor 1(TNFR I) gene expression [14, 15]. However, the nature and characteristics of the cytotoxic effect of SM and mechanisms of cell death induction remain to be elucidated. In this report, we demonstrate that SM mediates its cytotoxicity via oncosis.

Materials and methods

Cell lines and reagents

The human myelogenous leukemia K562 cell line and its multidrug-resistant counterpart K562/A02, squamous cell carcinoma KB cells and its multidrug-resistant counterpart KB/VCR, human prostate cancer PC3, human breast adenocarcinoma cell line MCF-7, and a normal cell line, human retinal pigment epithelial (RPE) 1 cell were maintained in RPMI 1640 medium (Hyclone, Logan, USA) supplemented with 10% fetal bovine serum (TBD, Tianjin, China) and 1% penicillin–streptomycin. The cells were cultured at 37°C with 5% CO_2.

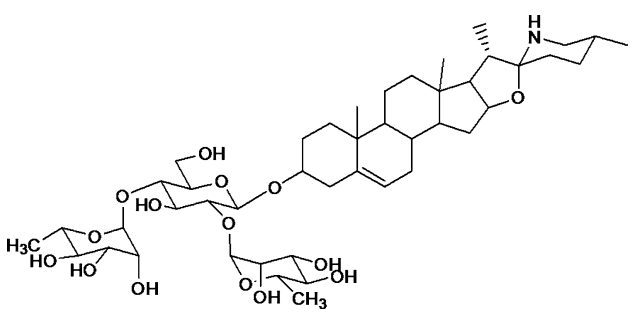

Fig. 1 The structure of solamargine

SM was isolated from *Solanum incanum*, a Chinese medicinal plant, in the authors' group and its purity was over 98% as measured by HPLC. The compound was initially dissolved in dimethyl sulfoxide (DMSO) at a concentration of 10 mM for in vitro assays and diluted to working concentrations with medium. 3-(4, 5-Dimethylthiazol)-2 and 5-diphenyltetrazolium bromide (MTT) were purchased from Sigma Co., USA. All other chemicals used in the experiments were commercial products of reagent grade.

MTT assay

Anticancer activity of SM was determined using MTT assay as previously reported (13). Cells were seeded at 5×10^3 cells/well in 96-well plate 24 h before drug treatment. Cells were treated with various concentrations of either SM or DMSO (0.1%, vol/vol). Following 24-h incubation with drug, 10 µl of 5 mg/ml solution MTT reagent was added to each well and incubated for 4 h. After centrifugation of the microtiter plates (1,200 *g*, 20 min) and removing the supernatant, 150 µl of dimethyl sulfoxide was added to dissolve the formazan crystals that remained in the wells. The absorbance was determined using microplate reader (Bio-Rad 680) at 570 nm. Wells containing DMSO were used for control cell viability and represented 100% cell survival, and wells without cells for blanking the spectrophotometer. IC_{50} values for each cell line were evaluated at a dose of drug causing 50% absorbance reduction in comparison with DMSO-treated control cells.

Lactate dehydrogenase (LDH) release assay

The LDH assay (Keygen Biotech. Co., Ltd, Nanjing, China) was performed according to the manufacturer's protocol. Briefly, cells seeds in microtiter plates were incubated with various concentrations of SM or vehicle at 37°C. As a control for maximum LDH release, cells were treated with 1% triton-X-100 (Sigma) in RPMI 1640 medium for 10 min before running the assay. To determine the normal LDH release, cells were cultured in serum-free medium. After centrifugation of the microtiter plates, 100 µl of the cell-free culture supernatants was transferred into new eppendorf tube. As the instruction of manufacturer's protocol, the spectrophotometric absorbance was determined using the microplate reader (Bio-rad 680) at 450 nm wavelength. The cytotoxicity detection assay was repeated in triplicate.

260 nm absorbing material release study

Leakage of cytoplasmic contents is a characteristic indication of damage to the cytoplasmic membrane [17]. Absorbance at 260 nm was used to estimate the amount of intracellular contents leaked from cells subjected to different concentrations of SM. The samples were filtered to remove the cells. OD at 260 nm was recorded. The percentage increase in OD_{260} of the SM-treated samples was compared with the control.

Propidium iodide (PI) uptake

Cell membrane integrity of SM-treated cells was also assessed by monitoring the uptake of the fluorescent probe, PI (Sigma, St Louis, Missouri, USA). It is a membrane impermeant nuclear stain and is used as an indicator for determining the cell membrane integrity [18]. For determining the PI uptake, cell suspensions of the control and SM-treated samples were centrifuged (1,700 *g*, 2 min) and the pellets were resuspended in PBS. The cell suspensions were incubated with PI (5 μg/ml) at 37°C for 15 min in the dark. Cells were washed twice following staining to remove the unbound PI. An aliquot of these suspensions was placed on the coverslip and observed under an inverted fluorescence microscope (Olympus IX71; Olympus Co., Tokyo, Japan) using 40× objective. PI-stained cells were viewed using 546 nm excitation and 620 nm emission filters. Both phase-contrast and fluorescent images were recorded using a cooled CCD camera.

Time-lapse microscopy

Cells were plated overnight in 35-mm culture dishes in RPMI 1640. Images were taken every 5 s by Olympus IX71 microscopy with an oil-immersion objective lens (PlanApo 40×, NA 1.40) in temperature-controlled box to keep temperature at 37°C. All subsequent analyses and processing of images were performed with Image-Pro Plus 6.0 software (Media Cybernetics, Silver Spring, USA).

Western blotting assay

The cell lysates were resolved by 12% SDS–PAGE and electrotransferred onto a nitrocellulose membrane followed by incubation with corresponding primary antibodies, including β-tubulin and actin at 1:1,000 dilutions overnight at 4°C. Secondary antibodies were used at 1:1,000 dilutions for 1 h at room temperature. Visualization was performed using the chemiluminescence method as described previously [19]. GAPDH was used as internal reference.

Immunofluorescence microscopy observation

KB cells seeded on 12-mm round glass coverslips and placed at the bottom of 12-well plates. After experimental treatment, cells on glass coverslips were fixed with cold methanol/acetone (1:1) for 5 min followed by immunostaining for β-tubulin and actin using rabbit anti-β-tubulin antibody and phalloidin as described previously [20]. DNA was counterstained with DAPI (1 μg/ml) for 5 min at room temperature. The samples were mounted on microscope slides with mounting medium and analyzed by fluorescence microscopy. The fluorescence images were processed using AutoQuant X 2.1 software from Cybernatics, Inc. (Bethesda, USA).

Determination of intracellular ATP concentration

We measured the amount of available intracellular ATP in cancer cell lines as an indirect parameter of the activity of $V–H^+$-ATPases. We used a commercially available ATP determination kit (Beyotime institute of Biotechnology) based on luciferase activity, following the instructions of the manufacturer.

Cell-cycle analysis

We used a FACScan flow cytometer (Becton–Dickinson, San Jose, CA) equipped with a 488-nm argon-ion laser. For cell-cycle analysis, asynchronous cells were cultured in the presence of different concentrations of SM. On incubation, the cells were harvested and washed in PBS, fixed in 70% cold ethanol overnight at 4°C, washed again in PBS, and incubated for 1 h in PBS containing 100 μg/ml RNase (Sigma) and 50 μg/ml PI. Ten thousand events per sample were acquired for data analysis using CELL-QUEST software by selective gating to exclude doublet cells. The results of the DNA content were modeled using ModFit (VERITY Software House, Inc., Topsham, ME).

Results

SM showed potent, rapid cytotoxic activity against human cancer cells

First, we studied the cytotoxic effect of SM on K562, KB cells, PC3, and MCF-7 by MTT assay. Exposure of K562 cells to the highest concentration of SM, 10 μM, induced 50% cell death quickly after 5 min, exposure for longer periods (24 h) at a dose of 10 μM led to about 80% cell death. The IC_{50}s of K562, KB, PC3, and MCF-7 were 8.0, 7.8, 5.9, and 8.2 μM, respectively. We next examined the cytotoxicity of SM in two MDR-expressing sublines:

K562/A02 and KB/VCR. The IC_{50}s of K562/A02 and KB/VCR were 5.4 and 7.1 μM, respectively. Expression of MDR1 gene, which encodes the P-glycoprotein responsible for extrusion of and resistance to multiple drugs, did not significantly alter the activity of SM against the multidrug-resistant human myelogenous leukemia cells and squamous cell carcinoma. When compared with the tumor cell lines, SM had a lower cytotoxicity on the normal cell RPE1 with an IC_{50} value of 23.4 μM.

Integrity of cell membrane

Based on the determination of LDH activity released from the cytosol of damaged cells into the medium, we evaluated the effect of SM on cell membrane integrity. No release of LDH into the medium was observed in vehicle-treated cells. After a 10-min treatment, SM at a concentration of 7.5 μM caused 45.7 and 59.3% cell death for K562 and KB, respectively (Fig. 2a). SM is thus a fast-acting toxin in killing cancer cells. In addition, we measured the leakage of cytoplasmic contents by measuring the OD at 260 nm. After 15 and 30 min treatment on KB and K562 cells, respectively, the OD_{260} of filtrates from cells suspensions were significantly increased (Fig. 2b).

The integrity of the cell membrane was also determined by the uptake of the DNA intercalating fluorescent dye PI. PI passes the cell membranes which were damaged by SM and intercalates into the DNA. This was visualized by fluorescence microscopy. As shown in Fig. 2c, the membrane of untreated cells was integrity, showed a normal and smooth morphology, and unstained by PI. However, cells incubated with SM showed a disrupted membrane and stained by PI.

SM induces membrane blebs

SM rapidly induced dramatic changes in the morphology of K562 and KB cells. Figure 3a shows time-lapse images of cells observed by phase-contrast microscopy. The blebs of K562 cells occur within 50 s of stimulation and last as long as 6 min, while the blebs of KB cells occur earlier within 35 s of stimulation and last only 2 min. Blebs were not found in vehicle-treated cells (data not shown).

Blebbing is independent of calcium and inhibited by polyethylene glycols (PEGs)

Chelating extracellular calcium with 5 mM EGTA did not prevent blebbing after a 27-min delay, showing that the formation of blebs does not depend on the influx of calcium (Fig. 3b). Blebbing was also not affected when the intracellular calcium concentration was clamped by the cell-permeable chelator BAPTA-AM (Fig. 3b).

We attempted to use PEGs of various molecular weights, which have been used to size large channels. Figure 3c shows the effects of PEGs on KB cell membrane bleb induced by 10 μM SM. PEGs having molecular

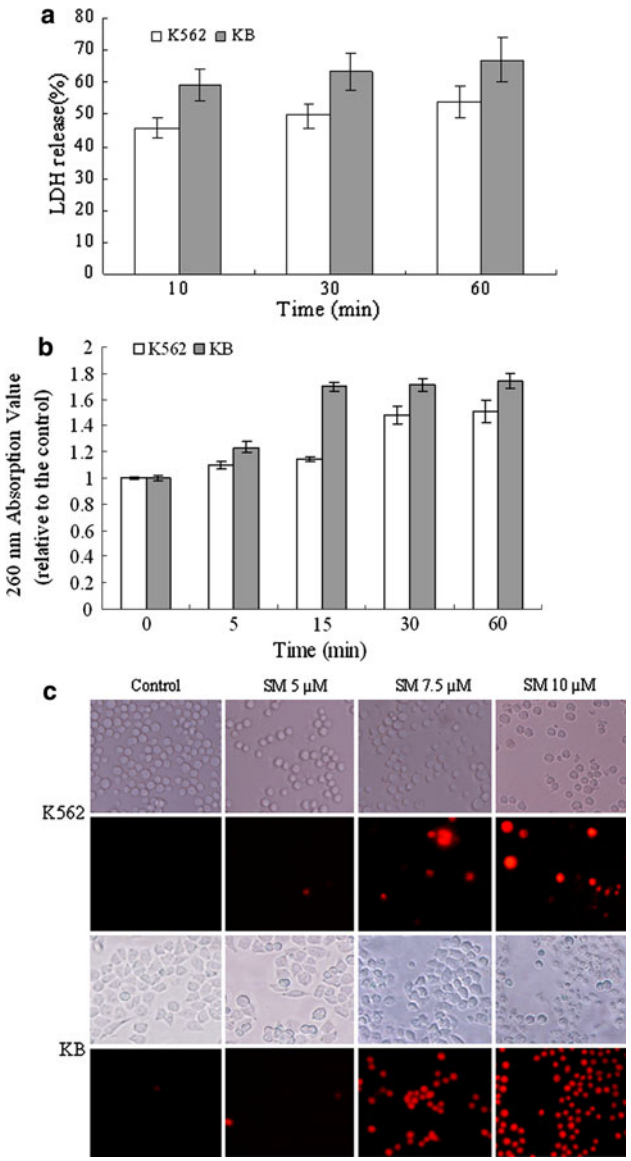

Fig. 2 **a** LDH release from cells subjected to 10 μM SM treatment. **b** Time-dependent release of 260 nm absorbing cellular materials from KB and K562 subjected to 10 μM SM. Data points represent mean and standard deviation of three experiments. **c** Morphological changes and PI uptake of K562 and KB cells after SM treatment

Fig. 3 **a** Time-lapse analysis of cell membrane blebs formation induced by 10 μM SM. **b** Effect of EGTA (5 mM) and BAPTA/AM (30 μM) on KB cell membrane blebs induced by 10 μM SM. **c** Effects of PEGs on KB cell membrane blebs induced by 10 μM SM. Points are the means of 100 cells; standard errors of the means are omitted for clarity. **d** Effect of PEGs and SM (10 μM) on inhibition of the proliferation of KB cell ▶

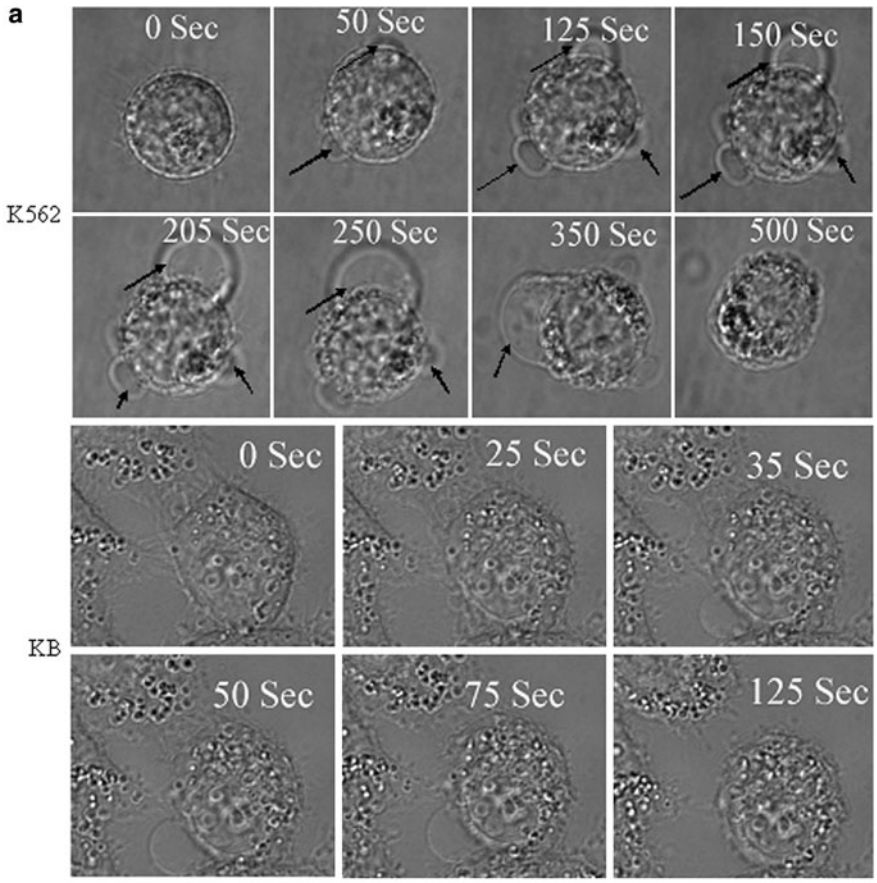
a
K562
0 Sec
50 Sec
125 Sec
150 Sec
205 Sec
250 Sec
350 Sec
500 Sec
KB
0 Sec
25 Sec
35 Sec
50 Sec
75 Sec
125 Sec

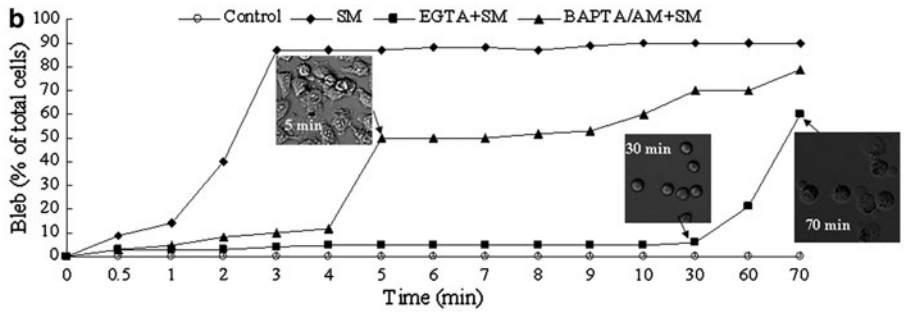
b
Control
SM
EGTA+SM
BAPTA/AM+SM
Bleb (% of total cells)
Time (min)
5 min
30 min
70 min

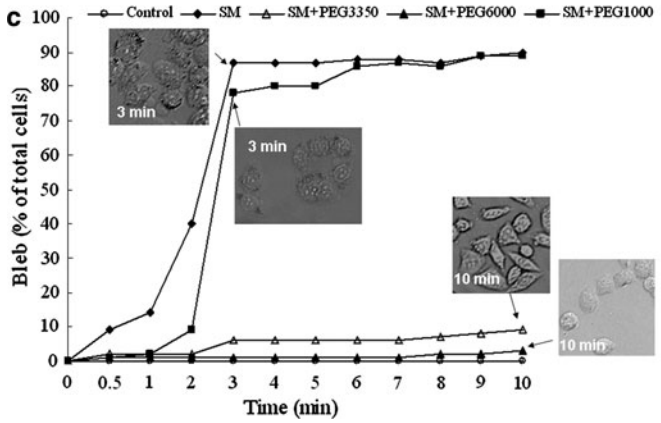
c
Control
SM
SM+PEG3350
SM+PEG6000
SM+PEG1000
Bleb (% of total cells)
Time (min)
3 min
3 min
10 min
10 min

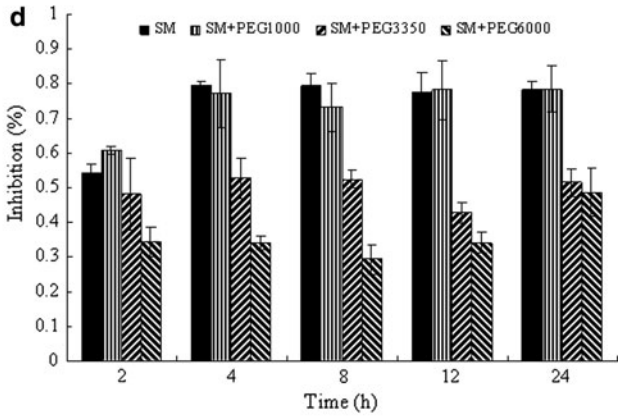
d
SM
SM+PEG1000
SM+PEG3350
SM+PEG6000
Inhibition (%)
Time (h)

weights ≥3,350 inhibited the membrane blebbing. The smaller molecular weight PEG 1,000 could not retard membrane blebbing. We also evaluated the effects of PEGs of various molecular weights on antitumor effect of SM. PEG 1,000 had no effect on antitumor effect of SM, while PEG 3,350 and 6,000 had the potential to reduce antitumor effect of SM (Fig. 3d).

ATP determination

ATP depletion can cause depolymerization of actin, breakdown of the actomyosin network, a change in lipid order of the plasma membrane, and membrane blebs. After addition of 5, 7.5, and 10 μM SM, ATP decreased to 79.3, 57, and 47% within 2 h, respectively (Fig. 4). ATP depletion can convert cell death from apoptosis morphology to a necrotic morphology, suggesting that intracellular ATP levels regulate the mode of cell death.

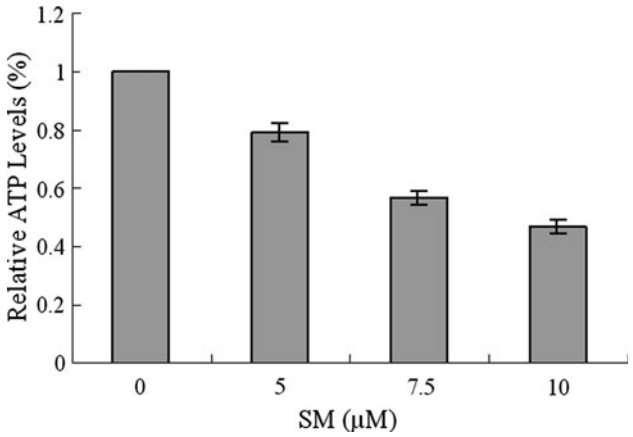

Fig. 4 The levels of intracellular ATP were decreased after treated by SM. Cells were treated as indicated and harvested, and total intracellular ATP content was measured

SM induced a rapid and profound alteration of cell architecture

In KB cells, SM exposure leads to a rapid, dramatic disruption of the normal architecture. As shown in Fig. 5a, intact microtubules arrays could be observed in untreated cells. However, during treatment with increasing concentration of SM, microtubules networks were decreased and short microtubules fragments were observed in the cytoplasm. We further observed simultaneous formation of actin stress fibers in SM-treated cells (Fig. 5b). To further confirm SM's ability to destroy microtubules and actin both in cultured cells, we used Western blot assay to detect the related protein. Immunoblotting of treated cell lysates displayed a decrease in β-tubulin and actin protein (Fig. 5c).

SM does not cause cell-cycle arrest

We further examined the effects of SM on cell-cycle progression using a flow cytometry procedure. K562 cells were used in our study to explore the general effects of SM on human tumors. K562 cells were cultured with 7.5 or

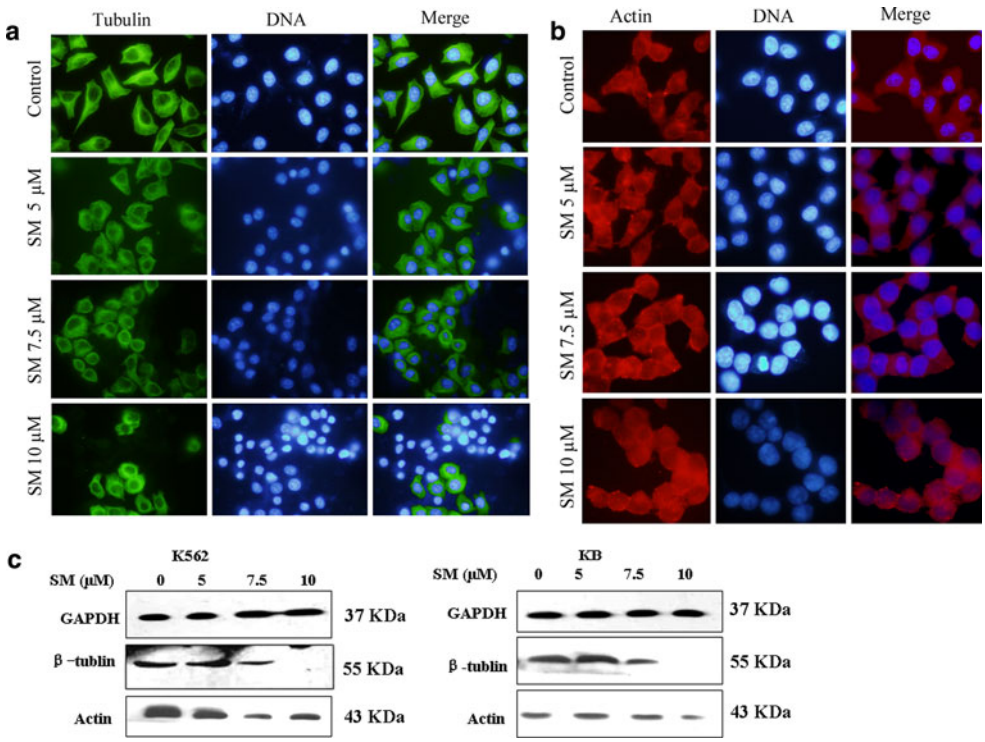

Fig. 5 Effect of SM on the microtubule (**a**) and actin (**b**) distribution in KB cells analyzed by a fluorescent microscope at magnification of 1,000×. **c** Expression level of β-tubulin and actin of K562 and KB cells after treated with or without SM

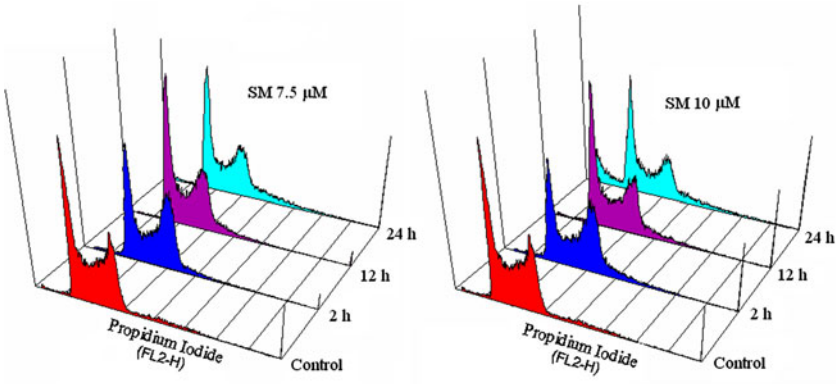

Fig. 6 SM does not induce cell-cycle arrest. K562 cells were incubated in the presence or absence of SM and at the indicated times were harvested and stained with PI

10 µM SM for 2, 12, and 24 h and then collected for flow cytometry assay. The results showed that SM does not cause cell-cycle arrest (Fig. 6).

Discussion

The patterns of cellular reaction to injury leading to cell death are important in the understanding and recognition of toxic and other types of injury. Apoptosis and oncosis, two types of prelethal reactions, have been characterized [1–3, 5–7]. The factors that determine which process occurs remain to be identified. In this work, we have examined the action of SM, an antitumor agent of steroidal alkaloidal saponins. SM showed potent cytotoxic activity against all tested types of tumor cells, and its action is not affected by the common multi-drug resistant mechanism. This action is triggered very rapidly and does not cause cell-cycle arrest. Soon after exposure to SM, cells initiate a death process including marked swelling and a series of profound morphological alterations that affect many cytoplasm organelles and plasma membrane. These features are typical of the process named oncosis, a term describing the progression of cellular events leading to necrotic cell death [2, 3, 21]. The cellular architecture is greatly affected as early as 1–3 h after SM treatment. In our previous study, SM also drastically affected the lysosomes and mitochondria, causing loss of mitochondrial membrane potential and of lysosomal integrity (unpublished data). Whole-cell recording experiments verified that the cell died as a result of acute injury and bursting, suggesting oncosis. The alterations suggest changes in the osmotic balance of the cell, possibly as a result of damage to cellular membranes, which we are currently investigating. After cell swelling, the cells begin to leak cytoplasmic components. Inclusion of certain PEG in the incubation medium prevents cell swelling caused by pore-forming cytolysins [22, 23]. The ability of PEG-termed osmotic stabilizing or protecting agents to prevent cell swelling is proportional to their molecular weight and concentration in medium. It has been proposed that osmotic stabilizing agents prevent toxin-induced cell swelling by causing the medium to be hypertonic compared with cytoplasm. For this to occur, the molecular weight of the osmotic stabilizing agent must be high enough that it cannot pass through the toxin-formed pores into the cytoplasm, and the concentration of the agent in the medium must be sufficient to counterbalance the toxin-induced increase in intracellular osmotic pressure. Based on the assumption that pore-forming cytolysins act as molecular sieves, osmotic stabilizing agents have been used to estimate the size of toxin-formed transmembrane pores [24, 25]. We found that PEG $\geq$3,350 had certain effects on action of SM: it can block membrane blebs formation and lowered cytotoxicity. Calcium seems to play an important role in the physiological process of cell death and apoptosis [10, 26, 27]. An increase in intracellular calcium concentration was not necessary for blebs induced by SM. Both chelating extracellular calcium with EGTA and clamping intracellular calcium concentrations at very low levels with a high concentration of the cell-permeable chelator BAPTA-AM did not prevent blebbing. Taken together, these results indicated that SM treatment causes a primary and preferential disruption of cytoplasm architecture and plasma membrane.

Our results show that SM is a very potent cytotoxic drug that displays an unusual and interesting mode of action. Most anticancer drugs have been considered to induce apoptosis as a result of nuclear DNA damage, activation of membrane death receptors, or cytoskeletal alteration [28–31]. SM induced membrane blebs formation and bursting rapidly. These blebs may be a consequence of ATP depletion and the consequent cytoskeletal alterations and loss of volume control. A decrease in ATP occurs very rapidly after SM treatment. This seems to be most important in situation that leads to oncosis when compared to apoptosis. Oncosis is characterized by loss of volume

control with massive swelling of most intracellular compartment, often based on ATP deficiency but also related to direct damage to the plasma membrane.

It is reported that SM can cause apoptosis of human hepatoma, breast, and lung cancer cells [14, 15, 32, 33]. In this study, we demonstrated SM can also induce oncosis. It is likely that apoptosis can be induced by low doses of SM and oncosis by high doses; both types of cell death are induced by intermediate concentration of SM. More studies are needed to fully characterize the antitumor action of SM including the identification of its primary target, the precise molecular mechanism of cytoplasmic organelle damage or the basis for its preferential effect on tumor cells.

Acknowledgments This work was supported by grants from the National Natural Science Foundation of China (no. 30925038) and Shandong Provincial Foundation (6GG1102023).

References

1. Trump BE, Berezesky IK, Chang SH, Phelps PC (1997) The pathways of cell death: oncosis, apoptosis, and necrosis. Toxicol Pathol 25:82–88
2. Majno G, Joris I (1995) Apoptosis, oncosis, and necrosis an overview of cell death. Am J Pathol 146:3–13
3. Van Cruchten S, Van den Broeck W (2002) Morphological and biochemical aspects of apoptosis, oncosis and necrosis. Anat Histol Embryol 31:214–223
4. Marsden VS, Connor LO, O'Reilly LA, Silke J, Metcalf D, Ekert PG, Huang DCS, Cecconi F, Kuida K, Tomaselli KJ, Roy S, Nicholson DW, Vaux DL, Bouillet P, Adams JM, Strasser A (2002) Apoptosis initiated by Bcl-2-regulated caspase activation independently of the cytochrome c/Apaf-1/caspase-9 apoptosome. Nature 419:634–637
5. Crisby M, Kallin B, Thyberg J, Zhivotovsky B, Orrenius S, Kostulas V, Nilsson J (1997) Cell death in human atherosclerotic plaques involves both oncosis and apoptosis. Atherosclerosis 130:17–27
6. Suárez Y, González L, Cuadrado A, Berciano M, Lafarga M, Muñoz A (2003) Kahalalide F, a new marine-derived compound, induces oncosis in human prostate and breast cancer cells. Mol Cancer Ther 2:863–872
7. Walisser JA, Thies RL (1999) Poly (ADP-Ribose) polymerase inhibition in oxidant-stressed endothelial cells prevents oncosis and permits caspase activation and apoptosis. Exp Cell Res 251:401–413
8. Ohno M, Takemura G, Ohno A, Misao J, Hayakawa Y, Minatoguchi S, Fujiwara T, Fujiwara H (1998) "Apoptotic" myocytes in infarct area in rabbit hearts may be oncotic myocytes with DNA fragmentation. Circulation 98:1422–1430
9. Takeda M, Shirato I, Kobayashi M, Endou H (1999) Hydrogen peroxide induces necrosis, apoptosis, oncosis and apoptotic oncosis of mouse terminal proximal straight tubule cells. Nephron 81:234–238
10. Trump BF, Berezesky IK (1996) The role of altered $[Ca^{2+}]_i$ regulation in apoptosis, oncosis, and necrosis. Biochim Biophys Acta 1313:173–178
11. Hall CA, Hobby T, Cipollini M (2006) Efficacy and mechanisms of α-solasonine and α-solamargine-induced cytolysis on two strains of *Trypanosoma cruzi*. J Chem Ecol 32:2405–2416
12. Ikeda T, Tsumagari H, Honbu T, Nohara T (2003) Cytotoxic activity of steroidal glycosides from solanum plants. Biol Pharm Bull 26:1198–1201
13. Ji YB, Gao SY, Ji CF, Zou X (2008) Induction of apoptosis in HepG2 cells by solanine and Bcl-2 protein. J Ethnopharmacol 115:194–202
14. Cham BE (2008) Cancer intralesion chemotherapy with solasodine Rhamnosyl glycosides. Res J Biol Sci 3:1008–1017
15. Hsu SH, Tsai TR, Lin CN, Yen MH, Kuo KW (1996) Solamargine purified from solanum incanum Chinese herb triggers gene expression of human TNFR I which may lead to cell apoptosis. Biochem Biophys Res Commun 229:1–5
16. Chang LC, Tsai TR, Wang JJ, Lin CN, Kuo KW (1998) The rhamnose moiety of solamargine plays a crucial role in triggering cell death by apoptosis. Biochem Biophys Res Commun 242:21–25
17. Leung WW, Keung WM, Kong YC (1976) The cytolytic effect of cobra cardiotoxin on ehrlich ascites tumor cells and its inhibition by Ca^{2+}. Naunyn-Schmiedeberg's Arch Pharmacol 292:193–198
18. Wang KR, Yan JX, Zhang BZ, Song JJ, Jia PF, Wang R (2009) Novel mode of action of polybia-MPI, a novel antimicrobial peptide, in multi-drug resistant leukemic cells. Cancer Lett 278:65–72
19. Meng F, Cai X, Duan J, Matteucci MG, Hart CP (2008) A novel class of tubulin inhibitors that exhibit potent antiproliferation and in vitro vessel-disrupting activity. Cancer Chemother Pharmacol 61:953–963
20. Shi YQ, Zhu CJ, Yuan HQ, Li BQ, Gao J, Qu XJ, Sun B, Cheng YN, Li S, Li X, Lou HX (2009) Marchantin C, a novel microtubule inhibitor from liverwort with anti-tumor activity both in vivo and in vitro. Cancer Lett 276:160–170
21. Lemasters JJ, Nieminen AL, Tian Q, Trost LC, Elmore SP, Nishimura Y, Crowe RA, Cascio WE, Bradham CA, Brenner DA, Herman B (1998) The mitochondrial permeability transition in cell death: a common mechanism in necrosis, apoptosis and autophagy. Biochim Biophys Acta 1366:177–196
22. Virginio C, MacKenzie A, North RA, Surprenant A (1999) Kinetics of cell lysis, dye uptake and permeability changes in cells expressing the rat $P2X_7$ receptor. J Physiol 519:335–346
23. Parsegian VA, Rand RP, Rau DC (1995) Macromolecules and water: probing with osmotic stress. Methods Enzymol 259:43–94
24. Parsegian VA, Bezrukov SM, Vodyanoy I (1995) Watching small molecules move: interrogating ionic channels using neutral solutes. Biosci Rep 15:503–514
25. Desat SA, Rosenberg RL (1997) Pore size of the malaria parasite's nutrient channel. Proc Natl Acad Sci USA 94:2045–2049
26. Bano D, Young KW, Guerin CJ, LeFeuMe R, Rothwell NJ, Naldini L, Rizzuto R, Carafoli E, Nicotera P (2004) Cleavage of the plasma membrane Na^+/Ca^{2+} exchanger in excitotoxicity. Cell 120:275–285
27. Schwab BL, Guerini D, Bano D, Ferrando-May E, Fava E, Tam J, Xu D, Xanthoudakis S, Nicholson DW, Carafoli E, Nicotera P (2002) Cleavage of plasma membrane calcium pumps by caspases: a link between apoptosis and necrosis. Cell Death Differ 9:818–831
28. Oh SH, Lee BH (2004) A ginseng saponin metabolite-induced apoptosis in HepG2 cells involves a mitochondria-mediated pathway and its downstream caspase-8 activation and Bid cleavage. Toxicol Appl Pharmacol 194:221–229
29. Paquet C, Sané AT, Beauchemin M, Bertrand R (2005) Caspase- and mitochondrial dysfunction-dependent mechanisms of lysosomal leakage and cathepsin B activation in DNA damage-induced apoptosis. Leukemia 19:784–791
30. Kaufmann SH (1999) Induction of endonucleolytic DNA cleavage in human acute myelogenous leukemia cells by etoposide,

camptothecin, and other cytotoxic anticancer drugs: a cautionary note. Cancer Res 49:5870–5878
31. Hsiang YH, Liu LF (1988) Identification of mammalian DNa topoisomerase I as an intracellular target of the anticancer drug camptothecin. Cancer Res 48:1722–1726
32. Shiu LY, Chang LC, Liang CH, Huang YS, Sheu HM, Kuo KW (2007) Solamargine induces apoptosis and sensitizes breast cancer cells to cisplatin. Food Chem Toxicol 45:2155–2164
33. Liu LF, Liang CH, Shiu LY, Lin WL, Lin CC, Kuo KW (2004) Action of solamargine on human lung cancer cells-enhancement of the susceptibility of cancer cells to TNFs. FEBS Lett 577:67–74